Human Cell (2018) 31:251–260
https://doi.org/10.1007/s13577-018-0208-z

RESEARCH ARTICLE

Atrial overexpression of microRNA-27b attenuates angiotensin II-induced atrial fibrosis and fibrillation by targeting ALK5

Yanshan Wang[1] · Heng Cai[2] · Hongmei Li[1] · Zhisheng Gao[1] · Kunqing Song[1]

Received: 5 February 2018 / Accepted: 10 April 2018 / Published online: 18 April 2018

Abstract

Atrial fibrosis influences atrial fibrillation (AF) development by transforming growth factor beta 1 (TGF-β1)/Smad pathway. Although microRNAs are implicated in the pathogenesis of various diseases, information regarding the functional role of microRNAs in atrial dysfunction is limited. In the present study, we found that microRNA-27b (miR-27b) was the dominant member of miR-27 family expressed in left atrium. Moreover, the expression of miR-27b was significantly reduced after angiotensin II (AngII) infusion. Masson's trichrome staining revealed that delivery of miR-27b adeno-associated virus to left atrium led to a decrease in atrial fibrosis induced by AngII. The increased expression of collagen I, collagen III, plasminogen activator inhibitor type 1 and alpha smooth muscle actin was also inhibited after miR-27b upregulation. In isolated perfused hearts, miR-27b restoration markedly attenuated AngII-induced increase in interatrial conduction time, AF incidence and AF duration. Furthermore, our data evidence that miR-27b is a novel miRNA that targets ALK5, a receptor of TGF-β1, through binding to the 3′ untranslated region of ALK5 mRNA. Ectopic miR-27b suppressed luciferase activity and expression of ALK5, whereas inhibition of miR-27b increased ALK5 luciferase activity and expression. Additionally, miR-27b inhibited AngII-induced Smad-2/3 phosphorylation without altering Smad-1 activity. Taken together, our study demonstrates that miR-27b ameliorates atrial fibrosis and AF through inactivation of Smad-2/3 pathway by targeting ALK5, suggesting miR-27b may play an anti-fibrotic role in left atrium and function as a novel therapeutic target for the treatment of cardiac dysfunction.

Keywords Atrial fibrosis · Atrial fibrillation · ALK5 · Smad · MicroRNA-27b

Introduction

Atrial fibrosis, which results in atrial fibrillation (AF), myocardial infarction or hypertension, is highly prevalent in heart failure [1, 2]. Multiple studies have evidenced the ability of angiotensin-inhibition for reducing atrial fibrosis and AF [2, 3]. One of the most common pathways governing angiotensin-mediated cardiac remodeling and fibrosis is the transforming growth factor beta (TGF-β) superfamily, in particular TGF-β1 [4, 5]. TGF-β1 binds with its heteromeric receptor complex consistent type I receptor/activin like kinase 5 (ALK5) and type II receptor (TGF-βRII) [4, 6]. The activation of ALK5 phosphorylates downstream effectors such as Smad-2 and Smad-3 and promotes their translocation into the nucleus, leading to transcription of pro-fibrotic genes [5, 7].

MicroRNAs (miRNAs) are a kind of endogenous, conserved, small (22 nucleotides in length) and noncoding RNAs that regulate the target genes post-transcriptionally by binding to the 3′ untranslated region (3′ UTR) [8]. Accumulating evidences have unveiled the critical role of miRNAs in the initiation and development of cardiovascular disease. For instance, plasma level of miR-208b has been suggested to be a diagnostic marker for myocardial infarction similar to troponine T [9, 10]. Circulating miR-483 was associated with the occurrence of postoperative AF [11]. Several studies have demonstrated higher level of miR-9, miR-374a, miR-454, miR-152 and miR-64 in AF patients and lower level of miR-99b, miR-150 and miR-328 [12–14], suggesting these miRNAs may be promising biomarkers for AF. Also, functional studies indicate that some miRNAs involve in atrial fibrosis and AF. Lu et al. reported that upregulation of

✉ Yanshan Wang
wangys_czch@126.com

[1] Department of Cardiology, Cangzhou Central Hospital, No. 201 Xinhua West Road, Yunhe District, Cangzhou 061000, Hebei, China

[2] Department of Cardiology, Tianjin Medical University General Hospital, Tianjin 300052, China

miR-328 with in vivo adenovirus reversed AF susceptibility in atrial tachypacing (A-TP) dogs [15]. Bernardo et al. demonstrated that inhibition of miR-154 with locked nucleic acid (LNA)-based anti-miR-154 was associated with less atrial fibrosis and improved cardiac function [16]. These findings suggest that manipulation of miRNA can be a promising therapeutic approach. In the current study, we provide the first evidence identifying miR-27b as an essential regulator of TGF-β1/ALK5/Smad-2/3 pathway, atrial fibrosis and AF by directly targeting ALK5. MiR-27b alleviated angiotensin II (AngII)-induced atrial fibrosis and arrhythmias. Our data indicate that miR-27b may be a novel therapeutic target for the treatment of cardiac pathologies associated with cardiac fibrosis and dysfunction.

Materials and methods

Materials and reagents

The adeno-associated virus (AAV) encoding miR-27b (AAV-27b) or GFP (AAV-GFP) were packaged into capsids from AAV-9 serotype by Oobio Company (Shanghai, China). Titers were 1.0×10^{13} viral genomes (vg)/ml. Angiotensin II (AngII), Masson's trichrome reagent, pentobarbital sodium and paraformaldehyde were obtained from Sigma (MA, USA). RPMI-1640 medium, fetal calf serum (FCS), penicillin, streptomycin, OptiMEM I medium and Lipofectamine 2000 were purchased from Invitrogen (CA, USA). Antibodies against ALK5, phospho-Smad-1, Smad-1, phospho-Smad-2/3, Smad-2/3 and GAPDH were obtained from Santa Cruz (CA, USA).

Animal experiments

8-week-old male wild-type C57BL/6 mice were obtained from the Jackson Laboratory (CA, USA) and housed in cages under a 12 h/12 h light–dark cycle with free access to water and to the diets. Before AngII infusion, mice were anesthetized with pentobarbital sodium (40 mg/kg, ip) and chest cavity was opened by an incision. The pericardium was carefully opened using ophthalmic tweezers. 1.0×10^{11} vg of AAV-GFP or AAV-27b in a final volume of 10 μl was injected into the pericardial space using a 36-gauge needle. After virus delivery, mice were implanted with an osmotic minipump (Alzet pumps Model 1002, Alzet, CA, USA) containing 200 μl of either phosphate buffered saline (PBS) or AngII at a dose of 2.0 mg/kg/day, for a period of 14 days. Sham-operated mice underwent the same procedure with the placement of osmotic minipumps containing PBS. All mice ($n=100$) were randomly divided into 4 groups: Sham ($n=40$), AngII ($n=40$), AngII AAV-GFP ($n=10$), AngII AAV-27b ($n=10$). According to the time points (1, 5, 10 and 14 days), the first two groups were further divided into 4 subgroups ($n=10$/group).

MiR-27b in situ hybridization

The probes for in situ hybridization of miR-27b and U6 were purchased from Exiqon (Vedbaek, Denmark). 4-μm tissue microarray (TMA) slides were prepared, deparaffinized, deproteinized, and pre-hybridized with hybridization buffer without probe. The hybridization was performed overnight in hybridization buffer with pre-denatured miR-27b or U6 probes. After washing, the slides were incubated with an alkaline phosphatase-conjugated anti-DIG Fab fragments (1:1500, Roche, IN, USA) and visualized for color detection.

Histological analysis of fibrosis

Mice were anesthetized with pentobarbital sodium and the whole hearts were excised. The tissues were immersed in 4% paraformaldehyde, embedded in paraffin, sliced into 5-mm-thick sections, and stained with Masson's trichrome. The photos were taken from the left atrium and analyzed using quantitative image analysis software (Image J 1.57, NIH, MD, USA) to compute the area of fibrosis as a percentage of the full left atrium area.

Quantitative polymerase chain reaction (qPCR)

Total RNA from left atrium was isolated using RNAeasy Mini Kit (Qiagen, NV, Netherlands) according to the manufacturer's instructions and determined by UV spectrometry. MiR-27a and miR-27b level was measured using TaqMan® Micro Assay Kit (Thermo Fisher Scientific, IL, USA). To measure the mRNA expression of collagen I, collagen III, plasminogen activator inhibitor type 1 (PAI-1) and alpha smooth muscle actin (α-SMA), total RNA was reverse-transcribed using a ReverTra ACE qPCR RT Kit (Toyobo, Osaka, Japan). qPCR reactions were performed with ABI 7500 Real-Time PCR System (Applied Biosystems, CA, USA) using Fast SYBR® Green Master Mix Kit (Applied Biosystems). The relative mRNA expression index was normalized with U6 or GAPDH. The primer sequences for qPCR of gene expression were as follows: collagen I, 5′-CTAGCCAACCGTGCTTCTCA-3′ and 5′-TTGGTCAGCACCACCAATGT-3′; collagen III, 5′-ACGTAAGCACTGGTGGACAG-3′ and 5′-GGAGGGCCATAGCTGAACTG-3′; PAI-1, 5′-AGCTTTGTGAAGGAGGACCG-3′ and 5′-CAGGGATGCAGACCCCAAAT-3′; α-SMA, 5′-CCTGGCCTAGCAACACTGAT-3′ and 5′-CGCAAGGCTTGATGCAAGTT-3′; ALK5, 5′-TAAAGACAACTGCCAGCCCT-3′ and 5′-CGCCTCCACGAGGTCATATT-3′; GAPDH, 5′-GGGCACGAAGGCTCATCATT-3′ and 5′-AGAAGGCTGGGGCTCATTTG-3′.

Echocardiography

On day 14, cardiac function was evaluated by transthoracic echocardiography (RMV 707B, Visual Sonics, ON, Canada). A 30-MHz linear array transducer was used to record the parasternal long- and short-axis views and guide M-mode analysis. The left ventricular fractional shortening (LVFS), left ventricular ejection fraction (LVEF), left ventricular end-diastolic diameter (LVDd), left ventricular end-systolic diameter (LVDs) and left ventricular posterior wall (LVPW) were determined.

Electrophysiological studies of perfused hearts

At the end of experimental period, ex vivo electrophysiological studies were performed in isolated perfused hearts using Langendorff apparatus as described previously [17, 18]. After dissecting the surrounding tissues, the hearts were stabilized for 10 min by perfusion via the aorta with a constant flow of Tyrode's solution (pH 7.4) containing 140 mM NaCl, 5.4 mM KCl, 2 mM $MgCl_2$, 1.8 mM $CaCl_2$, 10 mM glucose and 10 mM HEPES at 37 °C. A silver bipolar electrode was placed on the appendages of the left atrium and right atrium, and bipolar cardiac electrograms were recorded using a bio-amplifier system (PowerLab 8/30, AD Instruments, New South Wales, Australia). The effective refractory period (ERP) of the left atrium was determined by programmed atrial electrical stimulation with shortening of one extra S2 stimulus using 8 regularly paced beats with cycle lengths (CLs) of 90, 120 and 150 ms. The interatrial conduction time (IACT) was measured when the inter-electrode distance between left atrium and right atrium was set at 10 mm. AF inducibility was examined by S3 extrastimulus pacing method, of which the intervals of S1–S2 and S2–S3 were the same.

Cell culture and miRNA transfection

HEK293T cells were obtained from the Cell Bank of Chinese Academy of Medical Science (Shanghai, China) and maintained in RPMI-1640 medium containing with 10% FCS, 100 U/ml penicillin and 100 U/ml streptomycin at 37 °C, 5% CO_2, and 95% O_2. For miRNA transfection, miR-27b mimics or miR-27b inhibitor, mimics negative control or inhibitor negative (Rio Biotechnology, Guangzhou, China) were diluted with OptiMEM I medium and transfected into cells with Lipofectamine 2000 according to supplier's instructions.

Luciferase assay

The predicted binding sites of ALK5 were retrieved using a computational mRNA target analysis database (http://www.microRNA.org). The 3′ UTR of ALK5, which contains the predicted binding site for miR-27b, was cloned into the pMIR vector (RiboBio Co., Ltd, Guangzhou, China), referred to as wild-type ALK5 3′ UTR. The mutant 3′ UTR of ALK5 gene by substitution of 5 bp from seed region of miR-27b was synthesized and inserted into the equivalent reporter vector. HEK293T cells (2×10^5/well) were seeded in 24-well plates and then cotransfected with luciferase reporter (ALK5 3′ UTR or mutant ALK5 3′ UTR) and miR-27b mimics or miR-27b inhibitor using Lipofectamine 2000 for 48 h. Luciferase activity were quantified using a dual luciferase reporter system (Promega, WI, USA) according to the manufacturer's protocols.

Western blotting analysis

The left atrium tissues or HEK293T cells were lysed in RIPA lysis buffer (Beyotime Institute of Biotechnology, Shanghai, China) containing 1% protease and phosphatase inhibitors (Pierce Biotechnology, IL, USA). Protein concentration of each sample was quantified using a bicinchoninic acid kit (BioRad, CA, USA). Equal proteins were electrophoresed on 8–10% SDS polyacrylamide gel and transferred to nitrocellulose membranes (Millipore, MA, USA). Blots were blocked with 5% skim milk in TBS and then incubated with primary antibodies. Afterwards, the membranes were washed with PBS three times and incubated with horseradish peroxidase (HRP)-conjugated secondary antibodies (Beyotime Institute of Biotechnology) for 1 h at room temperature. The membranes were exposed to enhanced chemiluminescence kit (Thermo Fisher Scientific) and quantified by Image J software.

Statistical analysis

Data were reported as mean value ± standard error of mean (SEM) and compared by two-tailed Student's *t* test or one-way ANOVA, followed by the Bonferroni multiple comparison test. Statistical analysis was performed by SPSS 18.0 software (SPSS Inc., IL, USA). $P<0.05$ was considered statistically significant.

Results

MiR-27b expression is decreased in left atrium by AngII

MiR-27 family comprises 2 miRNAs: miR-27a and miR-27b. qPCR results displayed that the expression of miR-27b was about fivefold higher than that of miR-27a in left atrium (Fig. 1a). MiR-27a expression in left atrium was not significantly influenced by AngII infusion (Fig. 1b). Interestingly,

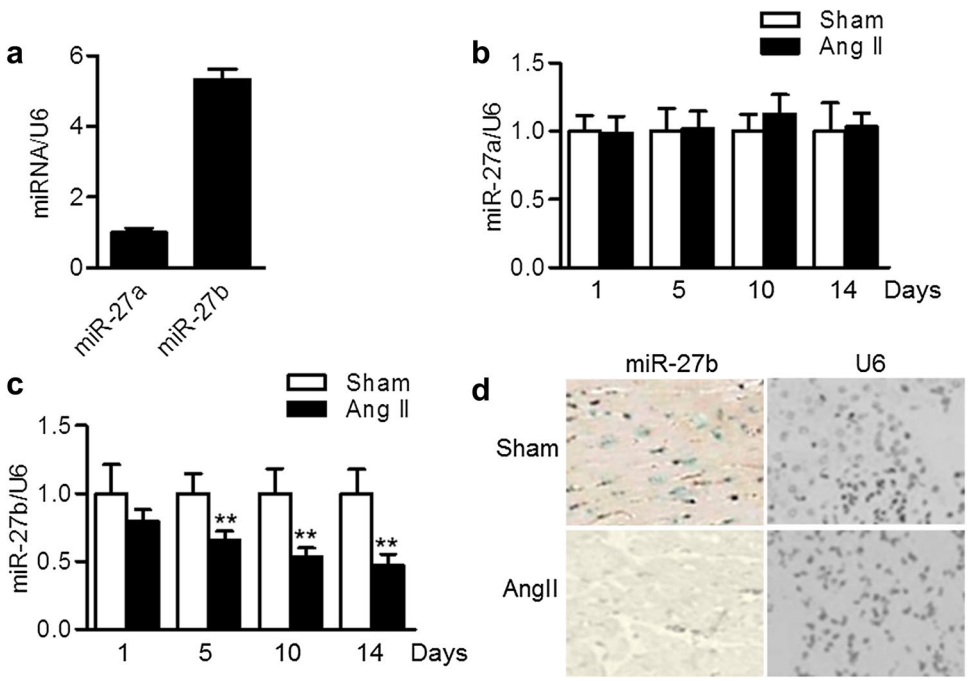

Fig. 1 Decreased expression of miR-27b in left atrium of AngII-treated mice. **a** qPCR analysis of miR-27a and miR-27b in left atrium. **b**, **c** C57BL/6 mice were infused with AngII at a dose of 2.0 mg/kg/day, for 1, 5, 10 and 14 days. The total RNA was isolated from left atrium, and the expression of miR-27a (**b**) miR-27b (**c**) was determined by qPCR. $^{**}P < 0.01$ vs. corresponding Sham group, $n = 5$. **d** Representative ISH staining images showing decreased miR-27b expression in left atrium after AngII treatment for 14 days compared with Sham group. The U6 was detected by ISH as an internal control

with regard to miR-27b expression, AngII infusion deceased miR-27b expression level by a time-dependent manner (Fig. 1c). Consistently, in situ hybridization analysis with miR-27b DIG probe also showed that the expression of miR-27b was significantly lower in left atrium of AngII-infused mice than those of Sham mice (Fig. 1d). These data suggest that the change of miR-27b may be associated with the pathogenesis of atrial fibrosis and AF.

Elevation of miR-27b expression blocks AngII-induced atrial fibrosis

To investigate the effects of miR-27b on the sequelae of AngII-induced atrial dysfunction, mice were infected with specific AAV encoding miR-27b followed by 14-day AngII infusion. Masson's trichrome staining of left atrium showed that AngII treatment significantly increased atrial fibrosis compared with Sham mice. However, miR-27b overexpression resulted in a reduction in atrial fibrosis (Fig. 2a, b). We next examined the expressions of collagen I, collagen III, PAI-1 and α-SMA, which are well known as important factors of heart fibrosis. qPCR analysis showed that AngII induced a marked increase in the mRNA expression of collagen I, collagen III, PAI-1 and α-SMA, which was inhibited by upregulation of miR-27b (Fig. 2c–f).

MiR-27b overexpression reduces atrial arrhythmias

Based on the inhibitory effects of miR-27b on atrial fibrosis, we subsequently aimed to determine the role of miR-27b in AF. The physiological and echocardiographic parameters are shown in Table 1. Compared with Sham mice, body weight was significantly lower in AngII-infused mice. AAV-27b had no effect on the loss of body weight. However, overexpression of miR-27b reversed AngII-induced increase of heart weight and the ratio of heart weight to body weight. Echocardiographic analysis showed that left ventricular fractional shortening, left ventricular ejection fraction and left ventricular end-systolic diameter remained unchanged among the 4 groups. AngII infusion led to concentric hypertrophy, evidenced by a decrease in left ventricular end-diastolic diameter and an increase in left ventricular posterior wall. No significant differences were observed between AngII-infused and AAV-27b-treated AngII-infused mice. In addition, there were also no significant differences in left-atrial effective refractory period among the 4 groups (Fig. 3a). But the interatrial conduction time was significantly increased in AngII-infused mice. This prolongation was attenuated after AAV-27b infection (Fig. 3b). In AngII-infused mice, the incidence of AF induced by S3 extrastimuli was 63% (5/8 mice). However, this incidence was decreased to 38% (3/8 mice) after AAV-27b infection (Fig. 3c). Moreover, AF duration was also shorter in 3 of 8 AAV-27b-treated AngII-infused mice compared with 5 of 8 AngII-infused mice (Fig. 3d).

MiR-27b directly targets at ALK5 3′ UTR

To understand the mechanism by which miR-27b protects against AngII-induced atrial fibrosis and AF, we used computational mRNA target analysis online software to search the potential target gene of miR-27b. The results showed

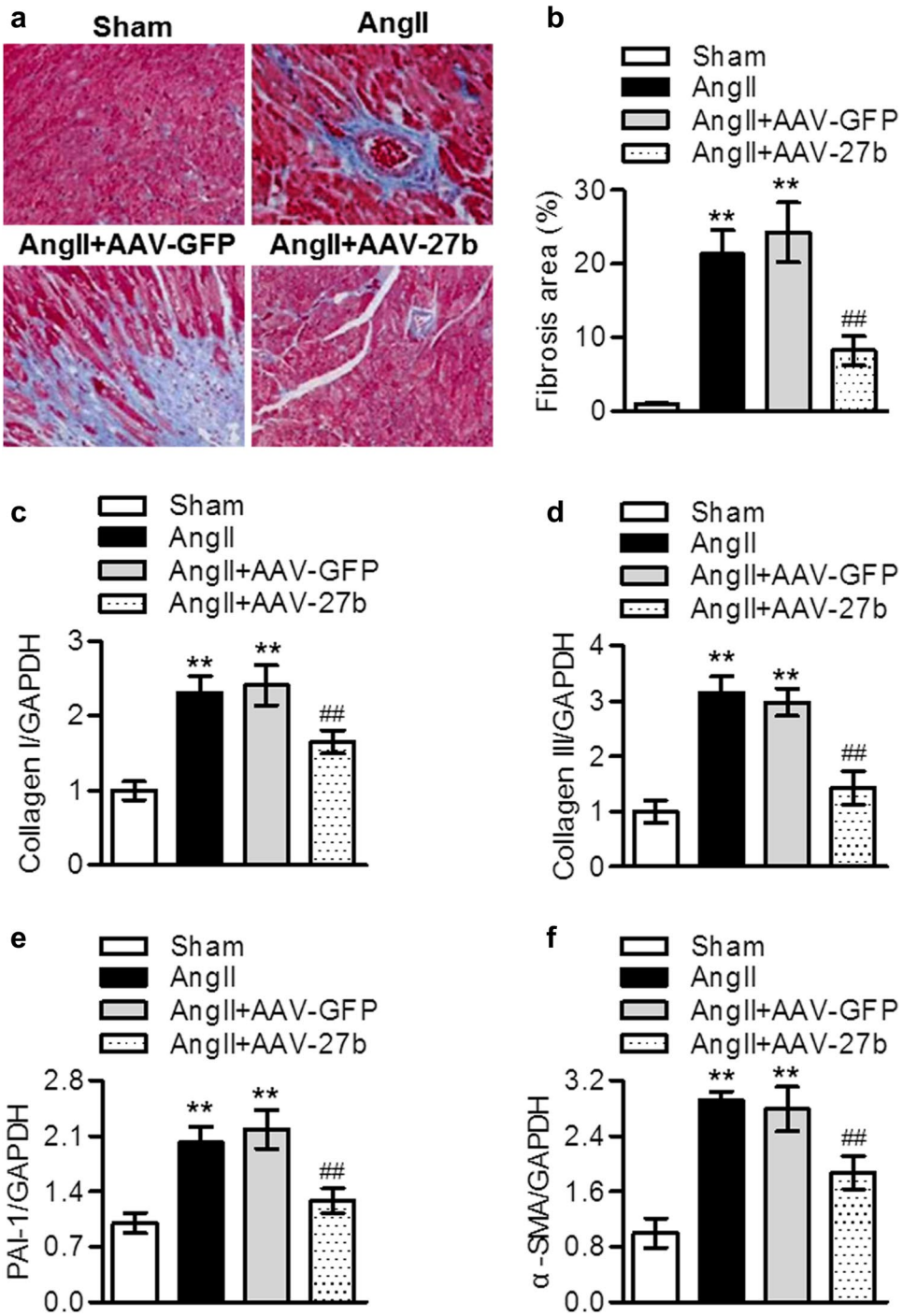

Fig. 2 MiR-27b upregulation ameliorates AngII-induced atrial fibrosis. **a** Mice were injected with adeno-associated virus (AAV) encoding miR-27b (AAV-27b) or GFP (AAV-GFP) followed by infusion of AngII for 14 days. Representative images revealed Masson's trichrome staining of left atrium each group. **b** The degree of myocardial fibrosis was determined by computer-based morphometric analysis. **c–f** qPCR analysis of the mRNA expression of collagen I (**c**), collagen III (**d**), PAI-1 (**e**) and α-SMA (**f**). $^{**}P<0.01$ vs. Sham; $^{\#\#}P<0.01$ vs. AngII, $n=6$

that ALK5, a gene known to be involved in the regulation of cardiac fibrosis, may be the target of miR-27b. A 8-bp fragment of ALK5 3′ UTR is complementary to the miR-27b seed sequence (Fig. 4a). By cotransfection with miR-27b mimics or miR-27b inhibitor and ALK5 3′ UTR luciferase reporter into HEK293T cells, the luciferase assay showed that overexpression of miR-27b decreased, while inhibition of miR-27b reduced the luciferase activity of ALK5 3′ UTR. When cells were transfected with the mutant ALK5 3′ UTR luciferase reporter, neither miR-27b mimics nor inhibitor influenced the luciferase activity (Fig. 4b, c). In agreement with the above observations, miR-27b mimics effectively decreased the mRNA expression of ALK5, whereas opposite results were obtained in cells transfected with miR-27b inhibitor (Fig. 4d, e). Furthermore, the effect of miR-27b on endogenous ALK5 protein expression was determined. Consistently, the protein expression of ALK5 after miR-27b mimics or inhibitor transfection showed the similar changes

Table 1 Physiological and echocardiographic parameters

Parameter	Sham	AngII		
		–	AAV-GFP	AAV-27b
Body weight (g)	25.6 ± 0.6	21.7 ± 1.4**	22.0 ± 0.9**	22.3 ± 0.8**
Heart weight (mg)	104.5 ± 1.9	145.1 ± 5.4**	152.3 ± 6.1**	134.2 ± 3.3##
Heart/body weight (mg/g)	4.1 ± 0.2	6.5 ± 0.3**	6.7 ± 0.5**	5.8 ± 0.2##
LVFS (%)	55.1 ± 1.7	52.3 ± 2.8	53.3 ± 0.6	51.5 ± 2.1
LVEF (%)	75.6 ± 0.9	76.4 ± 1.1	77.5 ± 1.5	76.7 ± 0.8
LVDd (mm)	3.13 ± 012	2.64 ± 0.11**	2.77 ± 0.24**	2.72 ± 0.18**
LVDs (mm)	1.62 ± 0.11	1.65 ± 0.22	1.71 ± 0.09	1.61 ± 0.14
LVPW (mm)	0.63 ± 0.08	0.89 ± 0.12**	0.84 ± 0.04**	0.86 ± 0.10**

LVFS left ventricular fractional shortening, *LVEF* left ventricular ejection fraction, *LVDd* left ventricular end-diastolic diameter, *LVDs* left ventricular end-systolic diameter, *LVPW* left ventricular posterior wall

**$P < 0.01$ vs. Sham; ##$P < 0.01$ vs. AngII, $n = 8$

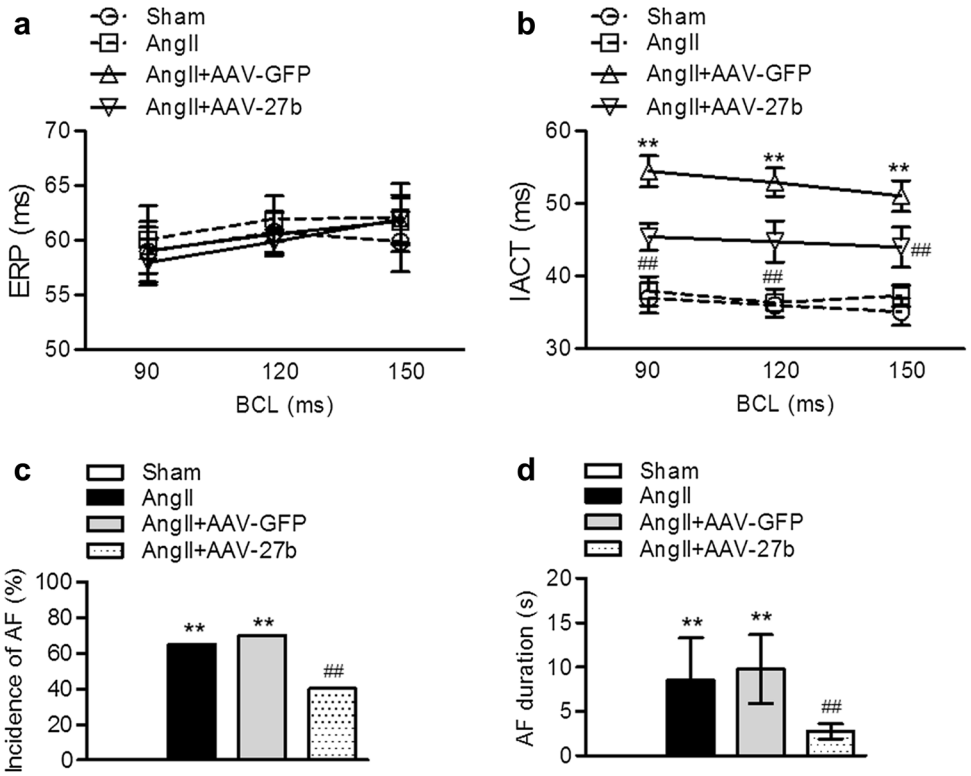

Fig. 3 Enforcing miR-27b expression inhibits atrial arrhythmias. **a**–**d** Electrophysiological study of isolated perfused hearts. Effective refractory period (ERP) (**a**), interatrial conduction time (IACT) (**b**), incidence of AF (**c**) and AF duration (**d**) were determined. *BCLs* basic cycle lengths. **$P < 0.01$ vs. Sham; ##$P < 0.01$ vs. AngII, $n = 8$

in the mRNA expression (Fig. 4f, g). These data indicate that miR-27b negatively regulates ALK5 expression.

MiR-27b upregulation inhibits activation of Smad-2/3 signaling

We next measured the activation of Smad signaling as downstream of ALK5. Although AngII caused a marked increase in Smad-1 phosphorylation, this phosphorylation level remained unchanged after AAV-27b infection (Fig. 5a, b). Of note, miR-27b overexpression inhibited AngII-induced increase of Smad-2/3 phosphorylation (Fig. 5c, d). These results suggest that miR-27b attenuates ALK5-Smad-2/3 signaling in AngII-induced atrial fibrosis and AF.

Discussion

The central finding of this study is that miR-27b was the only member of the miR-27 family that was significantly downregulated in left atrium from AngII-infused mice. In support, using gain-function strategy, we found that miR-27b ameliorated atrial fibrosis and AF by directly targeting ALK5, an effect that inhibited activation of Smad-2/3 signaling. Taken

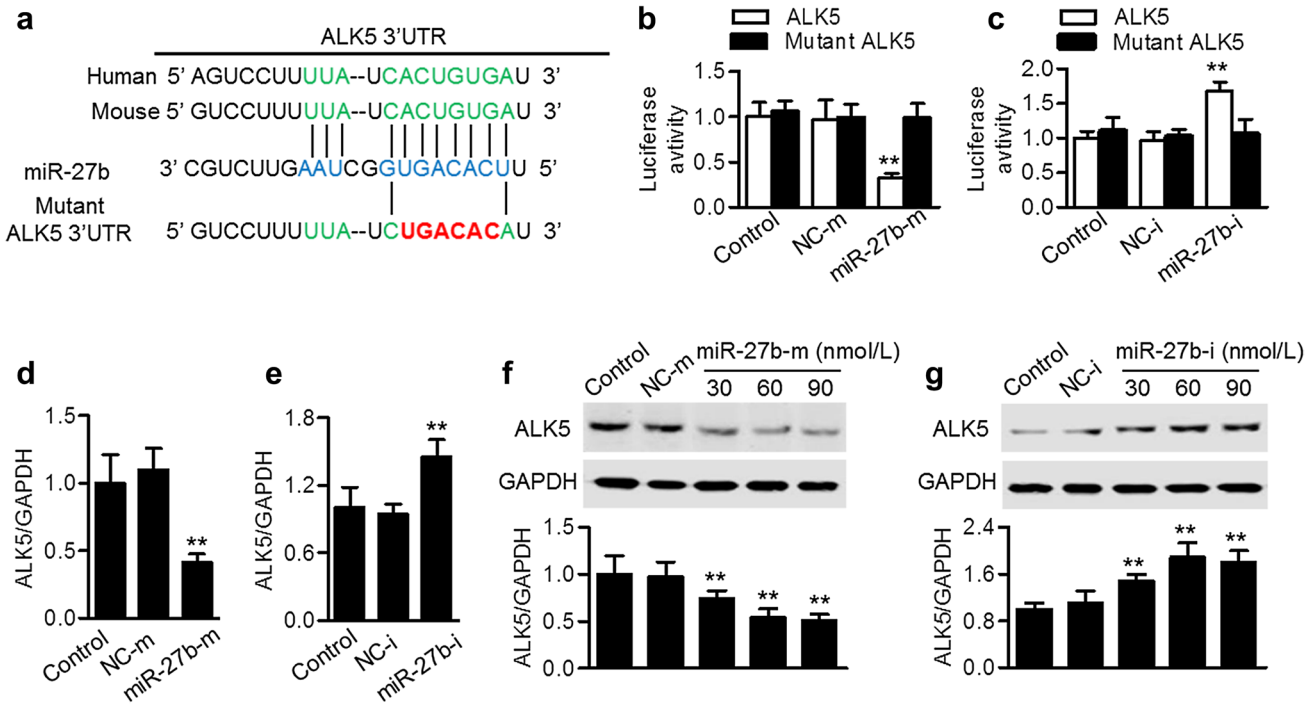

Fig. 4 MiR-27b directly targets ALK5 3′ UTR. **a** Predicted miR-27b seed matches to the sequence in the 3′ UTR of ALK5. **b**, **c** Dual luciferase activity assay was performed by co-transfection of luciferase reporter containing ALK5 3′-UTR or the mutant one with miR-27b mimics (miR-27b-m) (**b**) or miR-27b inhibitor (miR-27b-i) (**c**) in HEK293T cells. **d**, **e** qPCR analysis of ALK5 mRNA expression in cells transfected with miR-27b mimics (**d**) and miR-27b inhibitor (**e**) for 48 h. **f**, **g** The protein expression of ALK5 was determined by western blotting. $^{**}P<0.01$ vs. control, $n=6$

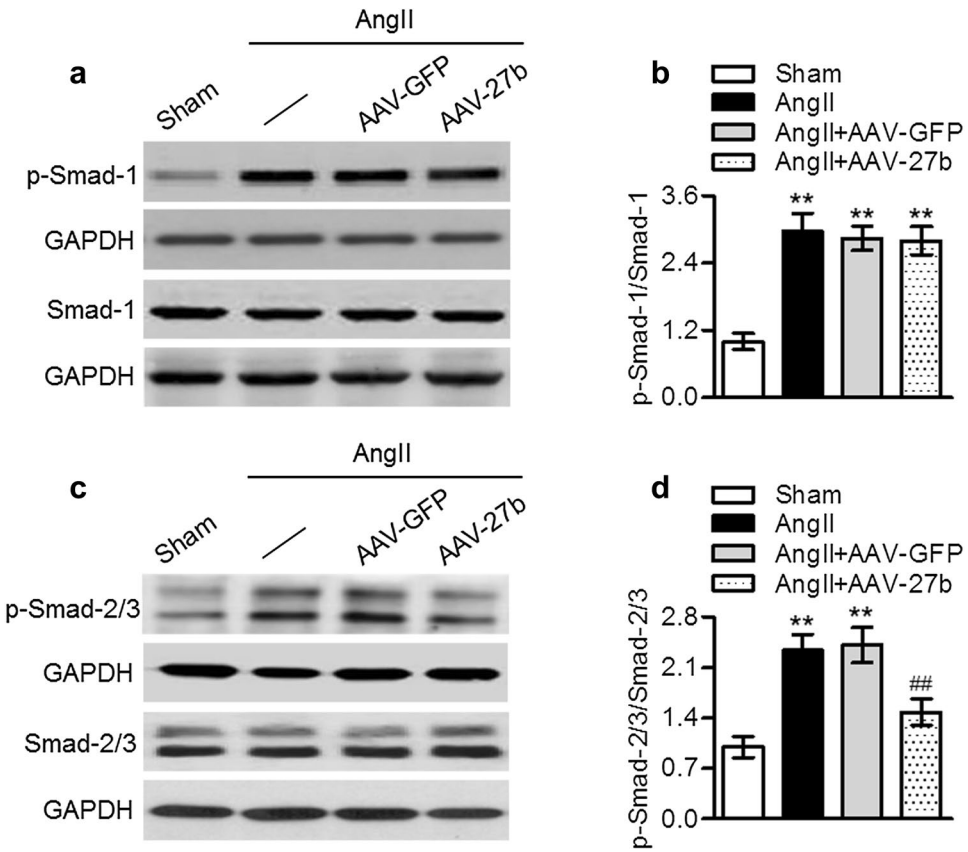

Fig. 5 MiR-27b overexpression attenuates AngII-induced Smad-2/3 signaling activation in left atrium. **a** Smad-1 phosphorylation and total Smad-1 protein expression were determined in left atrium isolated from Sham, AngII, and AngII-treated with AAV-GFP or AAV-27b. **b** Densitometric analysis of phosphorylated level of Smad-1. **c** Smad-2/3 phosphorylation and total Smad-2/3 protein expression were determined by western blotting. **d** Densitometric analysis of Smad-2/3 phosphorylation was performed. $^{**}P<0.01$ vs. Sham; $^{\#\#}P<0.01$ vs. AngII, $n=5$

together, our study indicates that miR-27b may serve as an important negative regulator of atrial fibrosis and AF.

In the last two decades, precise miRNA regulation is emerging as an important mechanism that involves in the pathogenesis of various diseases. Since several specific miRNAs expressions were found to be changed in cardiac hypertrophy and heart failure of experimental models, miRNA regulation was first described in 2006 in cardiovascular diseases [19]. Importantly, miRNAs are more stable than many mRNA moieties and even some proteins. Therefore, this stability has been indicated to exploit to function as a novel gene therapeutic approach in some diseases, including atrial fibrosis [8, 20]. MiR-27b belongs to the miR-27 family, which include 2 mature miRNAs: miR-27a and miR-27b. This miRNA family has been well recognized as an important regulator of cardiovascular events. MiR-27a/b overexpression was able to inhibit adipocytes differentiation, which is closely associated with the initiation of obesity [21, 22]. Furthermore, miR-27a/b regulated the metabolism of cellular cholesterol in THP-1 macrophages by targeting lipoprotein lipase and thus prevented atherosclerosis [23, 24]. With regard to cardiac function, miR-27b is cardioprotective and pro-angiogenic in a mouse model of myocardial infarction [20]. Previous study reported that miR-27b displayed an overt myocardial expression during heart development [25]. In the present study, we found that miR-27b is the dominant miR-27 family member expressed in left atrium. This result is consistent with the reports that miR-27b is highly expressed in the adult heart by microarrays [26, 27]. Interestingly, its expression was dramatically decreased after AngII infusion indicating a potential role of miR-27b atrial fibrosis and AF. Here, we investigated whether restoration of TIMP3 expression by local delivery of adenoviral in left atrium, could ameliorate AngII-induced atrial dysfunction. We found that elevation of TIMP3 attenuated AngII-induced atrial fibrosis, accompanied by inhibition of profibrotic genes expression. Moreover, the improvement in AF by miR-27b upregulation may be attributed to the reduced atrial fibrosis, it does not appear that these are regulated by normalizing left intra-atrial pressure because left ventricular end-diastolic diameter and left ventricular posterior wall remained unchanged after AngII infusion.

To investigate the mechanisms which allow miR-27b to ameliorate atrial fibrosis and AF in vivo, a computational mRNA target analysis database was used to predict the targets of miR-27b. The potential targets of miR-27b that could be involved in inflammation led us to focus on ALK5, also known as TGF-βRI, which regulates cardiac remodeling and fibrosis [6]. It has been well documented that TGF-β1 participates in the progressive remodeling of cardiac fibrosis and heart failure [5, 28, 29]. The pro-fibrotic effects of TGF-β1 are exerted via TGF-β1 receptors (ALK5 and TGF-βRII) and their downstream effector Smad signaling [7]. Therefore, ALK5 may be a promising target to block cardiac fibrosis. Increasing evidences have demonstrated that ALK5 regulates cardiac fibrosis via miRNA-dependent mechanism, as shown for miR-98, miR-22 and miR-101 [30–32]. In this study, we found an inverse regulation of ALK5 by miR-27b. Overexpression of miR-27b was associated with suppression of ALK5 expression and luciferase activity, whereas inhibition of miR-27b obtained opposite results. This data suggest that miR-27b directly targets the 3′ UTR of ALK5. In addition, our findings provide the evidences for the first time that miR-27b inhibited Smad-2/3 signaling by suppressing ALK5 expression. Overexpression of miR-27b did not affect AngII-induced Smad-1 phosphorylation, but was associated with inhibition of Smad-2/3 phosphorylation. These observations was in line with a previous study, in a certain extent, showing that lack of ALK1 expression decreased Smad1 activity without altering Smad3 activity after transverse aortic constriction [33]. Interestingly, a recent study found that independent of TGF-β1/ALK5 pathway, activation of activin A/ALK4 signaling also contributed to the pathogenesis of AngII-induced atrial fibrosis [34]. It is generally accepted that TGF-β1/ALK5 and activin A/ALK4 signaling pathways share the same downstream effectors, Smad-2/3 [35]. Thus, further study to clarify the different pathways such as activin A/ALK4 involved in the regulation of miR-27b in atrial fibrosis and AF is warranted.

In conclusion, miR-27b limits atrial fibrosis and AF through ALK5/Smad-2/3 signaling by targeting ALK5. These results reveal a novel anti-fibrotic role of miR-27b in left atrium, suggesting that miR-27b may be a promising therapeutic target for the treatment of cardiac dysfunction.

Compliance with ethical standards

Ethical standards All animal experiments were carried out according to the institutional guidelines from the Care and Use of Laboratory Animals of Cangzhou Central Hospital and were approved by the Institutional Animal Ethics Committee.

Conflict of interest The authors declare that they have no conflict of interest.

References

1. Roche PL, Filomeno KL, Bagchi RA, Czubryt MP. Intracellular signaling of cardiac fibroblasts. Compr Physiol. 2015;5(2):721–60. https://doi.org/10.1002/cphy.c140044.
2. Liu F, Levin MD, Petrenko NB, Lu MM, Wang T, Yuan LJ, Stout AL, Epstein JA, Patel VV. Histone-deacetylase inhibition reverses atrial arrhythmia inducibility and fibrosis in cardiac hypertrophy independent of angiotensin. J Mol Cell Cardiol. 2008;45(6):715–23. https://doi.org/10.1016/j.yjmcc.2008.08.015.
3. Li D, Shinagawa K, Pang L, Leung TK, Cardin S, Wang Z, Nattel S. Effects of angiotensin-converting enzyme inhibition on the development of the atrial fibrillation substrate in dogs with

ventricular tachypacing-induced congestive heart failure. Circulation. 2001;104(21):2608–14.
4. Leask A. Getting to the heart of the matter: new insights into cardiac fibrosis. Circ Res. 2015;116(7):1269–76. https://doi.org/10.1161/CIRCRESAHA.116.305381.
5. Massague J. TGFbeta signalling in context. Nat Rev Mol Cell Biol. 2012;13(10):616–30. https://doi.org/10.1038/nrm3434.
6. Doetschman T, Barnett JV, Runyan RB, Camenisch TD, Heimark RL, Granzier HL, Conway SJ, Azhar M. Transforming growth factor beta signaling in adult cardiovascular diseases and repair. Cell Tissue Res. 2012;347(1):203–23. https://doi.org/10.1007/s00441-011-1241-3.
7. Xu P, Liu J, Derynck R. Post-translational regulation of TGF-beta receptor and Smad signaling. FEBS Lett. 2012;586(14):1871–84. https://doi.org/10.1016/j.febslet.2012.05.010.
8. van den Berg NWE, Kawasaki M, Berger WR, Neefs J, Meulendijks E, Tijsen AJ, de Groot JR. MicroRNAs in atrial fibrillation: from expression signatures to functional implications. Cardiovasc Drugs Ther. 2017;31(3):345–65. https://doi.org/10.1007/s10557-017-6736-z.
9. Devaux Y, Mueller M, Haaf P, Goretti E, Twerenbold R, Zangrando J, Vausort M, Reichlin T, Wildi K, Moehring B, Wagner DR, Mueller C. Diagnostic and prognostic value of circulating microRNAs in patients with acute chest pain. J Intern Med. 2015;277(2):260–71. https://doi.org/10.1111/joim.12183.
10. Wang GK, Zhu JQ, Zhang JT, Li Q, Li Y, He J, Qin YW, Jing Q. Circulating microRNA: a novel potential biomarker for early diagnosis of acute myocardial infarction in humans. Eur Heart J. 2010;31(6):659–66. https://doi.org/10.1093/eurheartj/ehq013.
11. Harling L, Lambert J, Ashrafian H, Darzi A, Gooderham NJ, Athanasiou T. Elevated serum microRNA 483-5p levels may predict patients at risk of post-operative atrial fibrillation. Eur J Cardio Thorac Surg Off J Eur Assoc Cardio Thorac Surg. 2017;51(1):73–8. https://doi.org/10.1093/ejcts/ezw245.
12. Lu Y, Hou S, Huang D, Luo X, Zhang J, Chen J, Xu W. Expression profile analysis of circulating microRNAs and their effects on ion channels in Chinese atrial fibrillation patients. Int J Clin Exp Med. 2015;8(1):845–53.
13. Liu Z, Zhou C, Liu Y, Wang S, Ye P, Miao X, Xia J. The expression levels of plasma micoRNAs in atrial fibrillation patients. PLoS One. 2012;7(9):e44906. https://doi.org/10.1371/journal.pone.0044906.
14. McManus DD, Lin H, Tanriverdi K, Quercio M, Yin X, Larson MG, Ellinor PT, Levy D, Freedman JE, Benjamin EJ. Relations between circulating microRNAs and atrial fibrillation: data from the Framingham Offspring Study. Heart Rhythm. 2014;11(4):663–9. https://doi.org/10.1016/j.hrthm.2014.01.018.
15. Lu Y, Zhang Y, Wang N, Pan Z, Gao X, Zhang F, Zhang Y, Shan H, Luo X, Bai Y, Sun L, Song W, Xu C, Wang Z, Yang B. MicroRNA-328 contributes to adverse electrical remodeling in atrial fibrillation. Circulation. 2010;122(23):2378–87. https://doi.org/10.1161/CIRCULATIONAHA.110.958967.
16. Bernardo BC, Nguyen SS, Gao XM, Tham YK, Ooi JY, Patterson NL, Kiriazis H, Su Y, Thomas CJ, Lin RC, Du XJ, McMullen JR. Inhibition of miR-154 protects against cardiac dysfunction and fibrosis in a mouse model of pressure overload. Sci Rep. 2016;6:22442. https://doi.org/10.1038/srep22442.
17. Wakisaka O, Takahashi N, Shinohara T, Ooie T, Nakagawa M, Yonemochi H, Hara M, Shimada T, Saikawa T, Yoshimatsu H. Hyperthermia treatment prevents angiotensin II-mediated atrial fibrosis and fibrillation via induction of heat-shock protein 72. J Mol Cell Cardiol. 2007;43(5):616–26. https://doi.org/10.1016/j.yjmcc.2007.08.005.
18. Kume O, Takahashi N, Wakisaka O, Nagano-Torigoe Y, Teshima Y, Nakagawa M, Yufu K, Hara M, Saikawa T, Yoshimatsu H. Pioglitazone attenuates inflammatory atrial fibrosis and vulnerability to atrial fibrillation induced by pressure overload in rats. Heart Rhythm. 2011;8(2):278–85. https://doi.org/10.1016/j.hrthm.2010.10.029.
19. van Rooij E, Sutherland LB, Liu N, Williams AH, McAnally J, Gerard RD, Richardson JA, Olson EN. A signature pattern of stress-responsive microRNAs that can evoke cardiac hypertrophy and heart failure. Proc Natl Acad Sci USA. 2006;103(48):18255–60. https://doi.org/10.1073/pnas.0608791103.
20. Veliceasa D, Biyashev D, Qin G, Misener S, Mackie AR, Kishore R, Volpert OV. Therapeutic manipulation of angiogenesis with miR-27b. Vasc Cell. 2015;7:6. https://doi.org/10.1186/s13221-015-0031-1.
21. Zou B, Ge Z, Zhu W, Xu Z, Li C. Persimmon tannin represses 3T3-L1 preadipocyte differentiation via up-regulating expression of miR-27 and down-regulating expression of peroxisome proliferator-activated receptor-gamma in the early phase of adipogenesis. Eur J Nutr. 2015;54(8):1333–43. https://doi.org/10.1007/s00394-014-0814-9.
22. Sun L, Trajkovski M. MiR-27 orchestrates the transcriptional regulation of brown adipogenesis. Metab Clin Exp. 2014;63(2):272–82. https://doi.org/10.1016/j.metabol.2013.10.004.
23. Zhang M, Wu JF, Chen WJ, Tang SL, Mo ZC, Tang YY, Li Y, Wang JL, Liu XY, Peng J, Chen K, He PP, Lv YC, Ouyang XP, Yao F, Tang DP, Cayabyab FS, Zhang DW, Zheng XL, Tian GP, Tang CK. MicroRNA-27a/b regulates cellular cholesterol efflux, influx and esterification/hydrolysis in THP-1 macrophages. Atherosclerosis. 2014;234(1):54–64. https://doi.org/10.1016/j.atherosclerosis.2014.02.008.
24. Xie W, Li L, Zhang M, Cheng HP, Gong D, Lv YC, Yao F, He PP, Ouyang XP, Lan G, Liu D, Zhao ZW, Tan YL, Zheng XL, Yin WD, Tang CK. MicroRNA-27 prevents atherosclerosis by suppressing lipoprotein lipase-induced lipid accumulation and inflammatory response in apolipoprotein E knockout mice. PLoS One. 2016;11(6):e0157085. https://doi.org/10.1371/journal.pone.0157085.
25. Chinchilla A, Lozano E, Daimi H, Esteban FJ, Crist C, Aranega AE, Franco D. MicroRNA profiling during mouse ventricular maturation: a role for miR-27 modulating Mef2c expression. Cardiovasc Res. 2011;89(1):98–108. https://doi.org/10.1093/cvr/cvq264.
26. Hernandez-Torres F, Martinez-Fernandez S, Zuluaga S, Nebreda A, Porras A, Aranega AE, Navarro F. A role for p38alpha mitogen-activated protein kinase in embryonic cardiac differentiation. FEBS Lett. 2008;582(7):1025–31. https://doi.org/10.1016/j.febslet.2008.02.050.
27. Sayed D, Hong C, Chen IY, Lypowy J, Abdellatif M. MicroRNAs play an essential role in the development of cardiac hypertrophy. Circ Res. 2007;100(3):416–24. https://doi.org/10.1161/01.RES.0000257913.42552.23.
28. Lijnen PJ, Petrov VV, Fagard RH. Induction of cardiac fibrosis by transforming growth factor-beta(1). Mol Genet Metab. 2000;71(1–2):418–35. https://doi.org/10.1006/mgme.2000.3032.
29. Kuwahara F, Kai H, Tokuda K, Kai M, Takeshita A, Egashira K, Imaizumi T. Transforming growth factor-beta function blocking prevents myocardial fibrosis and diastolic dysfunction in pressure-overloaded rats. Circulation. 2002;106(1):130–5.
30. Cheng R, Dang R, Zhou Y, Ding M, Hua H. MicroRNA-98 inhibits TGF-beta1-induced differentiation and collagen production of cardiac fibroblasts by targeting TGFBR1. Hum Cell. 2017;30(3):192–200. https://doi.org/10.1007/s13577-017-0163-0.
31. Hong Y, Cao H, Wang Q, Ye J, Sui L, Feng J, Cai X, Song H, Zhang X, Chen X. MiR-22 may suppress fibrogenesis by targeting TGFbetaR I in cardiac fibroblasts. Cell Physiol Biochem Int J Exp Cell Physiol Biochem Pharmacol. 2016;40(6):1345–53. https://doi.org/10.1159/000453187.

32. Zhao X, Wang K, Liao Y, Zeng Q, Li Y, Hu F, Liu Y, Meng K, Qian C, Zhang Q, Guan H, Feng K, Zhou Y, Du Y, Chen Z. MicroRNA-101a inhibits cardiac fibrosis induced by hypoxia via targeting TGFbetaRI on cardiac fibroblasts. Cell Physiol Biochem Int J Exp Cell Physiol Biochem Pharmacol. 2015;35(1):213–26. https://doi.org/10.1159/000369689.
33. Morine KJ, Qiao X, Paruchuri V, Aronovitz MJ, Mackey EE, Buiten L, Levine J, Ughreja K, Nepali P, Blanton RM, Oh SP, Karas RH, Kapur NK. Reduced activin receptor-like kinase 1 activity promotes cardiac fibrosis in heart failure. Cardiovasc Pathol Off J Soc Cardiovasc Pathol. 2017;31:26–33. https://doi.org/10.1016/j.carpath.2017.07.004.
34. Wang Q, Yu Y, Zhang P, Chen Y, Li C, Chen J, Wang Y, Li Y. The crucial role of activin A/ALK4 pathway in the pathogenesis of Ang-II-induced atrial fibrosis and vulnerability to atrial fibrillation. Basic Res Cardiol. 2017;112(4):47. https://doi.org/10.1007/s00395-017-0634-1.
35. Hu J, Wang X, Wei SM, Tang YH, Zhou Q, Huang CX. Activin A stimulates the proliferation and differentiation of cardiac fibroblasts via the ERK1/2 and p38-MAPK pathways. Eur J Pharmacol. 2016;789:319–27. https://doi.org/10.1016/j.ejphar.2016.07.053.